

## Nonlinear Evolution of Current-Driven Instabilities and Energy Transport to Heavy Ions

TOIDA Mieko\*, SUGISHIMA Akihiro and OHSAWA Yukiharu  
*Department of Physics, Nagoya University, Nagoya 464-8602, Japan*

(Received: 5 December 2000 / Accepted: 18 August 2001)

### Abstract

Nonlinear evolution of current-driven instabilities is studied through theory and three-dimensional particle simulation, with special attention to associated potential formation and energy transport among different particle species. The plasma is assumed to consist of hydrogen (H) and helium (He) ions and electrons with the electron temperature higher than the ion temperatures. Electrons drift along a uniform magnetic field with an initial speed equal to the thermal speed,  $v_d = v_{Te}$ . It is found that the second harmonic H cyclotron wave with parallel phase velocity equal to  $v_d$  eventually becomes dominant, even though it is only marginal in the initial state. This wave produces a coherent potential profile and heats He ions more significantly than H ions.

### Keywords:

current-driven instability, ion cyclotron wave, ion acoustic wave, energy transport, multi-ion-species plasma

### 1. Introduction

Current-driven instabilities are believed to play essential roles in heavy-ion heating in space plasmas. For example, for  $^3\text{He}$  rich events in solar flares or for  $\text{O}^+$  heating in the Earth's ionosphere, cyclotron resonances with unstable waves are thought to be important, and several theoretical models have been proposed [1-5]. However, those studies are mainly based on linear theories and have not succeeded in quantitatively explaining observations. To do this, we need to make a theory which self-consistently treats both nonlinear evolution of instabilities and energy transport among different particle species.

In the previous paper [6], we studied current-driven instabilities using a two-dimensional, electrostatic, particle simulation code with full ion and electron dynamics. The plasma was assumed to consist of hydrogen (H) and helium (He) ions and electrons with the electron temperature higher than the ion

temperatures. The electrons drift along a uniform magnetic field with the initial speed equal to the thermal speed,  $v_d = v_{Te}$ . The linear theory for these initial conditions predicts that ion acoustic waves and H cyclotron waves are unstable, with the former having much greater growth rates. The simulations show that after the development of ion acoustic waves and H cyclotron waves, second harmonic H cyclotron waves are destabilized owing to the change in the electron parallel velocity distribution function,  $f_e(v_{||})$ . Even though they are only marginally unstable in the initial state, they eventually grow to the largest amplitudes and strongly influence energy transport.

In the previous two-dimensional simulation (2D), the number of unstable H cyclotron waves was small. In order to make a theory predicting the dominant wave, we must study the nonlinear evolution of the instabilities by the simulation where a large number of unstable

\*Corresponding author's e-mail: toida@phys.nagoya-u.ac.jp

waves are contained. In this paper, we develop a theory on nonlinear evolution of the instabilities. Furthermore, we study associated potential formation and ion heating by the three-dimensional simulation (3D) where the number of unstable H cyclotron waves is much larger than in 2D. It is shown that a second harmonic H cyclotron wave with phase velocity equal to the initial electron drift speed eventually becomes dominant and produces a coherent potential profile. The heating of He ions by the dominant wave is more noticeable than that of H ions.

## 2. Theory

Current-driven instabilities in a plasma consisting of H, He and electrons are studied with special attention to the effect of the change in the electron velocity distribution function. We assume that, initially, the ions have isotropic Maxwellian velocity distribution functions and the electrons drift along a uniform magnetic field with the speed  $v_d$ . The electron distribution function at time  $t = 0$  is taken to be

$$f(v_{\parallel}, v_{\perp}, 0) = \frac{1}{(2\pi v_{Te}^2)^{3/2}} \exp\left(-\frac{v_{\perp}^2}{2v_{Te}^2}\right) \exp\left(-\frac{(v_{\parallel} - v_d)^2}{2v_{Te}^2}\right), \quad (1)$$

The subscript  $\parallel$  and  $\perp$  denote quantities parallel and perpendicular to the magnetic field, respectively. We

study the initial value problem of this system.

We assume that the electron velocity distribution function at time  $t$  can be written as

$$f(v_{\parallel}, v_{\perp}, t) = \frac{1}{(2\pi v_{Te}^2)^{3/2}} \exp\left(-\frac{v_{\perp}^2}{2v_{Te}^2}\right) g(v_{\parallel}, t). \quad (2)$$

Then, growth rate of an ion acoustic wave is

$$\gamma(t) \approx \frac{\omega^3 \sqrt{\pi} v_{Te}}{k_{\parallel}^2 \sum_{i=H, He} \omega_{Di}^2 \Gamma_0(\mu_i) \lambda_{De}^2} \left[ \frac{\partial g}{\partial v_{\parallel}} \Big|_{v_{\parallel}=\omega/k_{\parallel}} - \sum_{i=H, He} \frac{\lambda_{De}^2}{\lambda_{Di}^2 v_{Te}} \frac{\omega \Gamma_0(\mu_i)}{k_{\parallel} v_{Ti}} \exp\left(-\frac{\omega^2}{2k_{\parallel}^2 v_{Ti}^2}\right) \right], \quad (3)$$

and frequency  $\omega$  is

$$\omega = \lambda_{De} \sum_{i=H, He} [\omega_{pi}^2 \Gamma_0(\mu_i)]^{1/2} k_{\parallel}. \quad (4)$$

Here, the subscript  $i$  refers to ion species;  $k$  is the wave number;  $\lambda_{De}$  and  $\lambda_{Di}$  are the electron and ion Debye lengths, respectively; and  $\Gamma_n(\mu_i)$  is  $\Gamma_n(\mu_i) = I_n(\mu_i) \exp(-\mu_i)$ , where  $I_n$  is the modified Bessel function of the  $n$ -th order. The quantity  $\mu_i$  is defined as  $\mu_i = k_{\perp}^2 \rho_i^2$  with  $\rho_i$  being the gyro-radius,  $\rho_i = v_{Ti}/\Omega_i$ .

The growth rate of  $n$ -th harmonic hydrogen cyclotron wave ( $n = 1, 2, \dots$ ) is

$$\gamma(t) \approx \alpha_n \left[ \frac{\partial g}{\partial v_{\parallel}} \Big|_{v_{\parallel}=\omega/k_{\parallel}} - \sum_{i=H, He} \sum_m \frac{\lambda_{De}^2}{\lambda_{Di}^2 v_{Te}} \frac{\omega \Gamma_m(\mu_i)}{k_{\parallel} v_{Ti}} \exp\left(-\frac{(\omega - m\Omega_i)^2}{2k_{\parallel}^2 v_{Ti}^2}\right) \right]. \quad (5)$$

Here,  $\omega$  and  $\alpha_n$  are given by

$$\omega = n\Omega_H \left\{ 1 + \Gamma_n(\mu_H) \left[ 1 - \Gamma_0(\mu_H) + \frac{n_e T_H}{n_H T_e} + \frac{n_{He} q_{He}^2 T_H}{n_H q_H^2 T_{He}} (1 - \Gamma_0(\mu_{He})) \right]^{-1} \right\}, \quad (6)$$

$$\alpha_n = \frac{v_{Te}}{\lambda_{De}^2} \left[ \frac{1}{\lambda_{DH}^2} \sum_m \frac{m \Omega_H \Gamma_m(\mu_H)}{(\omega - m\Omega_H)^2} + \frac{1}{\lambda_{DHe}^2} \sum_m \frac{m \Omega_{He} \Gamma_m(\mu_{He})}{(\omega - m\Omega_{He})^2} \right]^{-1}. \quad (7)$$

The parallel phase velocities of H cyclotron waves are larger than those of ion acoustic waves.

According to the simulations [6], the development

of the instabilities may be summarized as follows. When the electron temperature is higher than the ion temperatures, ion acoustic waves are initially most

unstable [7]. They grow firstly and flatten  $g(v_{\parallel})$  around their phase velocities, which makes the slope of  $g(v_{\parallel})$  steep in the region of phase velocities of H cyclotron waves. This increases the growth rates of H cyclotron waves. These waves further change the shape of  $g(v_{\parallel})$ , which destabilizes waves that were marginal in the initial state. The instabilities of waves with different phase velocities give rise to flattening of  $g(v_{\parallel})$  over a wide velocity region.

We now discuss what determines the wave that eventually becomes dominant. As we will see later in Fig. 2, simulations show that the second harmonic H cyclotron wave with  $\omega/k_{\parallel} \approx v_d$  grows to the largest amplitude, although it is marginal in the initial state. That the waves with  $\omega/k_{\parallel} \approx v_d$  are important after the development of the instabilities may be related to the fact that the difference  $g(v_{\parallel}, 0) - g(v_{\parallel}, t)$  is the largest at  $v_{\parallel} \approx v_d$ , as shown in Fig. 1. If we assume this, then we would be able to predict which harmonic wave becomes important, using the values of  $\alpha_n$  given by Eq. (7). That is, the  $n$ -th harmonic wave with the largest  $\alpha_n$  and with  $\omega/k_{\parallel} \approx v_d$  would eventually become dominant.

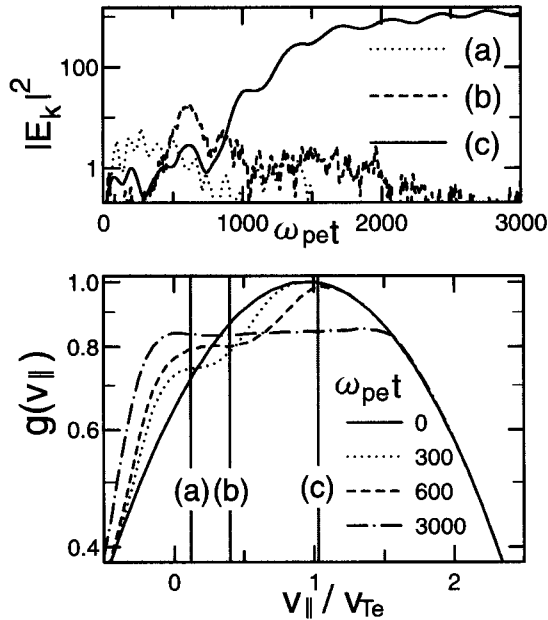


Fig. 1 Evolution of three typical modes and electron parallel velocity distribution function. Lines (a), (b) and (c) in the upper panel show an ion acoustic wave, fundamental and second harmonic H cyclotron waves, respectively. Their wave numbers are  $(k_{\parallel} \rho_H, k_{\perp} \rho_H) = (0.97, 0.21)$ ,  $(0.19, 0.42)$ , and  $(0.11, 0.73)$ , respectively. Three vertical lines in the lower panel represent their phase velocities.

The energy of the dominant wave is gradually transferred to some ions that satisfy resonance condition,  $\omega - n\Omega_i - k_{\parallel}v_{\parallel} \approx 0$ . If ions have isotropic Maxwell velocity distribution function, the increase rates of perpendicular kinetic energy densities can be given by

$$\frac{dK_{i\perp}}{dt} = \frac{\pi}{8} \frac{n_i q_i^2 \Gamma_n(\mu_i)}{m_i v_{Ti} k_{\parallel}} \exp\left(-\frac{(n\Omega_i - \omega)^2}{k_{\parallel}^2 v_{Ti}^2}\right) |E|^2, \quad (8)$$

where  $n_i$  is the ion density and  $E$  is the electric field.

### 3. Simulation

We have performed simulations using a three-dimensional, electrostatic particle code with full ion and

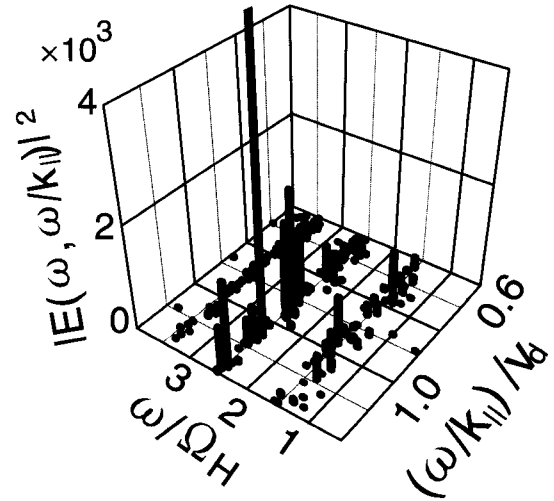


Fig. 2 Power spectrum of fundamental, second and third harmonic H cyclotron waves as a function of the frequency,  $\omega$ , and phase velocity,  $\omega/k_{\parallel}$ .

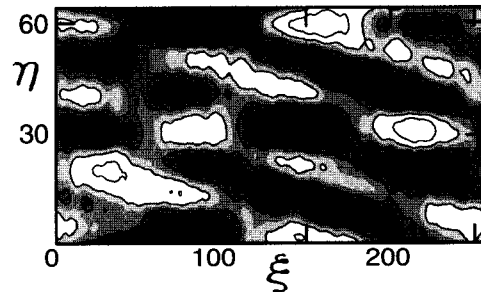


Fig. 3 Contour map of electric potential at  $\omega_{pe} t = 4800$ .  $\xi$  and  $\eta$  are lengths parallel and perpendicular to the magnetic field, respectively.

electron dynamics. A  $128 \times 256 \times 16$  grid is used in the  $x, y, z$  direction with periodic boundary conditions. The grid size is the Debye length  $\lambda_{De}$ . We chose a uniform magnetic field such that  $(B_x, B_y, B_z) = B_0(0.089, 0.49, 0.87)$ . This configuration enables us to have ion acoustic waves and a large number of H cyclotron waves; the number of H cyclotron waves in this 3D system is about ten times as large as that in the previous 2D system [6]. The particle numbers are  $N_e = 33, 554, 432$ ,  $N_H = 27, 787, 264$ , and  $N_{He} = 2, 883, 584$ . The mass ratios are  $m_H/m_e = 100$  and  $m_{He}/m_H = 4$ ; the charge ratios are  $q_H/|q_e| = 1$  and  $q_{He}/q_H = 2$ ; the temperature ratios are  $T_e/T_H = 5.0$  and  $T_{He}/T_H = 1$ ; the electron cyclotron frequency is  $|\Omega_e|/\omega_{pe} = 2.0$ . The initial electron drift speed is equal to the electron thermal speed,  $v_d = v_{Te}$ .

For these initial conditions, the linear theory predicts that ion acoustic waves, fundamental and second harmonic H cyclotron waves are unstable, while He cyclotron waves are stable [6]. The ion acoustic waves have the greatest growth rates. The second harmonic waves have only small initial growth rates, compared with the ion acoustic waves and the fundamental waves (see Fig. 1–3 in ref. [6]). However, the values of  $\alpha_n$  given by Eq. (7) for the second harmonic waves are larger than those for the fundamental waves;  $\alpha_2 \sim (3/2)\alpha_1$  for the waves with  $\omega/k_{||} = v_d$ .

We show in Fig. 1 time variations of the amplitudes of three typical modes and electron parallel velocity distribution function  $g(v_{||})$ . Here the electric field energies  $|E_k|^2$  are normalized to  $m_e v_{Te}^2$ . Dotted line (a) in the upper panel represents an ion acoustic wave with  $(k_{||}\rho_H, k_{\perp}\rho_H) = (0.97, 0.21)$ . Dashed line (b) and solid line (c) show fundamental and second harmonic H cyclotron waves with  $(k_{||}\rho_H, k_{\perp}\rho_H) = (0.19, 0.42)$  and  $(0.11, 0.73)$ , respectively. The vertical three lines in the lower panel show phase velocities,  $\omega/k_{||}$ , of these three modes. Note that mode (c) has the phase velocity,  $\omega/k_{||}$ , equal to  $v_d$  and is only marginal in the initial state. It is destabilized after the development of modes (a) and (b), and grows to a much larger amplitude than the other two modes. Because of the interaction with these waves,  $g(v_{||})$  eventually has a large plateau region,  $0 \leq v_{||}/v_{Te} \leq 1.5$ .

Figure 2 shows spectrum of H cyclotron waves as a function of the frequency and phase velocity. Fundamental, second, and third harmonic waves are plotted. The spectrum is obtained from all components of the electric field for the period from  $\omega_{pe}t = 0$  to 6000. The highest peak is at  $\omega/\Omega_H \approx 2.4$  and  $(\omega/k_{||})/v_d \approx 1.0$ .

This is mode (c). The second harmonic wave with  $\omega/k_{||} \approx v_d$  eventually becomes dominant in 3D system as well as in 2D system, although the numbers of unstable modes are quite different in these two systems. This simulation result supports the theory developed in this paper.

The dominant wave produces a coherent potential profile. Figure 3 shows a contour map of the electric field potential at  $\omega_{pe}t = 4800$ . Here,  $\xi$  and  $\eta$  are the lengths parallel and perpendicular to the magnetic field, respectively. They are normalized to  $\lambda_{De}$ . We can clearly see the potential profile due to mode (c).

The electron drift energy is transferred to the ion energies through unstable modes; the total energy in the simulation is conserved. The energy transfer from mode (c) to He ions is noticeable. Figure 4 shows time variations of kinetic energies of H and He ions. The dashed and solid lines represent parallel and perpendicular energies, respectively. After mode (c) is destabilized, i.e., after  $\omega_{pe}t \approx 1500$ ,  $K_{\perp}$  of He ions continues to increase more rapidly than that of H ions. The heating of He ions is caused by the cyclotron resonance with mode (c). (The acceleration of He ions is not observed in the simulation.)

Figure 5 shows contour maps of the ion distribution functions in the  $(v_{||}, v_{\perp})$  plane. The velocities of H and He ions are normalized by  $v_{TH}$  and  $v_{THe}$ , respectively.

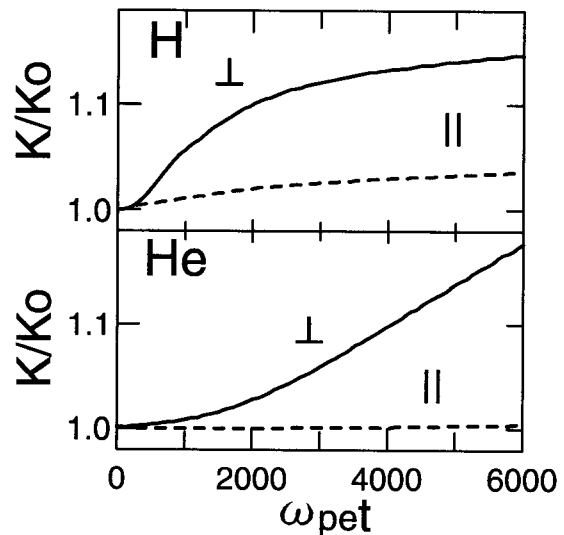


Fig. 4 Time variations ion kinetic energies. The dashed and solid lines show parallel and perpendicular energies, respectively. Energies are normalized to their initial values.

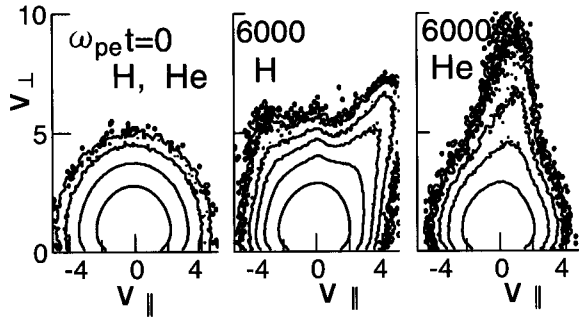


Fig. 5 Contour maps of  $f_H$  and  $f_{He}$  in the  $(v_{\parallel}, v_{\perp})$  plane.

The left panel shows the initial distribution functions; H and He ions have the same profile. The middle and right panels show  $f_H$  and  $f_{He}$  at  $\omega_{pe}t = 6000$ , respectively. The H ions with  $v_{\parallel}/v_{TH} \approx 4.0$  are heated perpendicularly. These particles satisfy the resonance condition  $\omega - 2\Omega_H - k_{\parallel}v_{\parallel} \approx 0$  with mode (c) ( $\omega = 2.4\Omega_H$ ,  $k_{\parallel}\rho_H = 0.11$ ). The He ions with  $v_{\parallel}/v_{THe} \approx 0.65$  are heated by the same wave, through the resonance  $\omega - 5\Omega_H - k_{\parallel}v_{\parallel} \approx 0$ . Because the resonance takes place in the region of small parallel velocity, the time rate of change in  $K_{\perp}$  of He is much greater than that of H for  $\omega_{pe}t \gtrsim 1500$ , as expected from Eq. (8).

#### 4. Summary

We have studied current-driven instabilities in a plasma consisting of H, He and electrons through theory and three-dimensional particle simulation, with attention to nonlinear evolution of instabilities and energy transport among different particle species. It is found that the second harmonic H cyclotron wave with parallel phase speed equal to the electron drift speed  $v_d$  ( $\sim v_{Te}$ ) eventually becomes dominant and produces a coherent potential profile. The heating of He ions by the dominant wave is more noticeable than that of H ions.

#### References

- [1] L.A. Fisk, *Astrophys. J.* **224**, 1048 (1978).
- [2] M. Ashour-Abdalla and H. Okuda, *J. Geophys. Res.* **89**, 2235 (1984).
- [3] T.X. Zhang, M. Toida and Y. Ohsawa, *J. Phys. Soc. Jpn.* **62**, 2545 (1993).
- [4] T.X. Zhang and Y. Ohsawa, *Solar Physics* **158**, 115 (1995).
- [5] S. Nakazawa, T.X. Zhang and Y. Ohsawa, *Solar Physics* **166**, 159 (1996).
- [6] M. Toida, T. Maeda, I. Shiiba, A. Sugishima and Y. Ohsawa, *Phys. Plasmas* **7**, 4882 (2000).
- [7] J.M. Kindel and C.F. Kennel, *J. Geophys. Res.* **76**, 3055 (1971).